Frequency Dependence of Left-Handed and Right-Handed Periodic Transmission Structures

Douglas R. Jachowski and Clifford M. Krowne

Microwave Technology Branch, Electronics Science and Technology Division
Naval Research Laboratory, Washington, DC 20375

***Abstract* — Techniques from image-parameter filter theory are used to derive frequency dependent representations of the characteristic impedance, phase, and attenuation of some left-handed and right-handed periodic transmission structures, with implications for the design of artificial transmission lines composed of a finite number of cascaded unit-cell circuits.**

I. Introduction

Recent interest in left-handed materials and their uses in microwave and millimeter wave devices [1], [2] has prompted investigations into circuit analogs of intrinsic left-handed materials [3]. One example is the use of the well-known distributed backward-wave transmission line concept [4] in quasi-lumped element form to realize left-handed transmission lines on conventional planar substrates [5]. More generally, one current trend is to use periodic recurrent structures to realize a variety of filter-like artificial transmission lines [6]-[10].

The concept of artificial transmission lines formed from periodic and composite periodic structures is at least as old as filter theory itself, and a large body of knowledge exists on the analysis and design of such lines [11]-[17]. One objective of this paper is to apply this knowledge to review the frequency dependence of some of the lowest order left-handed and right-handed symmetric unit-cell circuits suitable as building blocks for periodic artificial lines. Another objective is to emphasize the relevance of image-parameter filter theory [11]-[17] to the design and analysis of periodic artificial lines, and to suggest that, when contemplating designing periodic structures with filter-like properties, it would be beneficial to consider designing non-periodic structures by means of modern filter synthesis (e.g., [18]), instead.

II. Analysis of Periodic Transmission Structures

A periodic transmission structure is a recurrent cascade of a unit-cell circuit and is ideally terminated in the image impedances of its ports, as shown in Fig. 1 [11]. Although unit cells need not be symmetric, reciprocal, and lossless, for convenience only such unit cells will be considered.

The properties of a periodic structure can be deduced from the properties of its unit cell. The characteristic impedance of the periodic artificial line is identical to the characteristic impedance (and image impedance) of its unit cell, while the phase constant of a periodic artificial line is equivalent to the phase constant of its unit cell compounded by the number of unit cells in the line. The transmission response of a periodic artificial line built from distributed-element unit cells typically exhibits repeating passbands and stopbands, sometimes termed a "band-gap" characteristic. Passbands occur at frequencies where the characteristic impedance is purely real, while band gaps occur at frequencies where the characteristic impedance is purely imaginary (i.e., at frequencies where the wave evanesces or disperses rather than propagates).

When a unit-cell has a ladder-like topology, the most convenient means of analysis is by *ABCD* matrices, [*T*], where the product of the [*T*] of the individual components forms the overall [*T*] of the unit cell [14]-[18]. For non-ladder-like unit-cell circuits, the most convenient means of analysis is by nodal analysis (summing the currents into each circuit node using Kirchhoff's Current Law and solving the simultaneous equations for the characteristic of interest) [19].

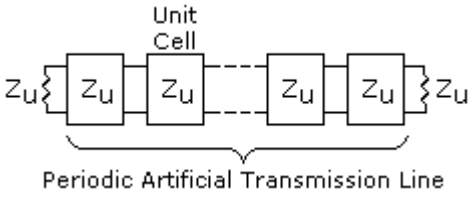

Fig. 1. A periodic artificial transmission line composed of a sequence of identical unit cells of characteristic impedance, Z_u, and with matched terminations, Z_u.

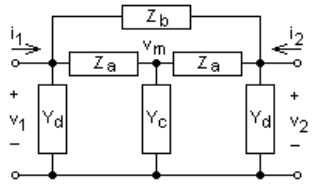

Fig. 2. Schematic of a composite Π-T unit cell.

Report Documentation Page

Form Approved
OMB No. 0704-0188

1. REPORT DATE	2. REPORT TYPE	3. DATES COVERED
JUN 2004		**00-00-2004 to 00-00-2004**

4. TITLE AND SUBTITLE	5a. CONTRACT NUMBER
Frequency Dependence of Left-Handed and Right-Handed Periodic Frequency Dependence of Left-Handed and Right-Handed Periodic Transmission Structures	5b. GRANT NUMBER
	5c. PROGRAM ELEMENT NUMBER
6. AUTHOR(S)	5d. PROJECT NUMBER
	5e. TASK NUMBER
	5f. WORK UNIT NUMBER
7. PERFORMING ORGANIZATION NAME(S) AND ADDRESS(ES) **Naval Research Laboratory,Microwave Technology Branch,Electronics Science and Technology Division,Washington,DC,20375**	8. PERFORMING ORGANIZATION REPORT NUMBER
9. SPONSORING/MONITORING AGENCY NAME(S) AND ADDRESS(ES)	10. SPONSOR/MONITOR'S ACRONYM(S)
	11. SPONSOR/MONITOR'S REPORT NUMBER(S)

12. DISTRIBUTION/AVAILABILITY STATEMENT
Approved for public release; distribution unlimited

13. SUPPLEMENTARY NOTES
2004 IEEE MTT-S International Microwave Symposium Digest, pp. 1831 - 1834 Vol.3, 6-11 June 2004.

14. ABSTRACT
Techniques from image-parameter filter theory are used to derive frequency dependent representations of the characteristic impedance, phase, and attenuation of some left-handed and right-handed periodic transmission structures, with implications for the design of artificial transmission lines composed of a finite number of cascaded unit-cell circuits.

15. SUBJECT TERMS

16. SECURITY CLASSIFICATION OF:			17. LIMITATION OF ABSTRACT	18. NUMBER OF PAGES	19a. NAME OF RESPONSIBLE PERSON
a. REPORT	b. ABSTRACT	c. THIS PAGE			
unclassified	**unclassified**	**unclassified**	**Same as Report (SAR)**	**4**	

Lowest-order symmetric unit cells with both series and shunt elements are composed of three lumped and/or distributed elements in either a "Π" ("mid-series") or "T" ("mid-shunt") configuration. For generality, the composite unit cell of Fig. 2 is analyzed and constraints are applied to determine the properties of specific circuits of interest.

Lossless distributed elements, whether highpass (e.g., waveguide) or lowpass (e.g., coaxial) in nature, can be modeled as symmetric Π-networks comprised of shunt admittances, $Y=j\ \tan(\theta/2)/Z_o$, connected by a series impedance, $Z=j\ Z_o\sin(\theta)$ [17], where Z_o and θ are the element's characteristic impedance and electrical length. Distributed elements simplify to equivalent shunt admittances of $j\ \tan(\theta)/Z_o$ when open circuited and $-j/(Z_o\ \tan(\theta))$ when short circuited. T-type unit cells with series-connected distributed elements have a cascaded-Π or "M"-type five-element equivalent circuit.

Results for many different three-element unit cells are provided in Table 1 (after [13] and [16]), and comparable aspects of the table entries are readily apparent.

A. The ABCD Matrix

Using nodal analysis, the elements of the ABCD matrix of the lossless reciprocal unit cell of Fig. 2 are

$$\begin{pmatrix} v_1 \\ i_1 \end{pmatrix} = \begin{pmatrix} A & B \\ C & D \end{pmatrix} \bullet \begin{pmatrix} v_2 \\ -i_2 \end{pmatrix}, \tag{1}$$

$$A = D = \left.\frac{v_1}{v_2}\right|_{i_2=0} = \frac{Z_b + Z_a(2 + Y_c Z_b + 2Y_d Z_b) + {Z_a}^2(Y_c + Y_c Y_d Z_b)}{2Z_a + Y_c {Z_a}^2 + Z_b}, \tag{2}$$

$$B = j\ B_I = \left.\frac{-v_1}{i_2}\right|_{v_2=0} = \frac{Z_a Z_b(2 + Y_c Z_a)}{2Z_a + Y_c {Z_a}^2 + Z_b}, \tag{3}$$

$$C = j\ C_I = \left.\frac{i_1}{v_2}\right|_{i_2=0} = \frac{(Y_c + 2Y_d + Y_c Y_d Z_a)(Z_b + Z_a(2 + Y_d Z_b)}{2Z_a + Y_c {Z_a}^2 + Z_b}. \tag{4}$$

Since the unit cell is assumed to be lossless, A, D, B_I, and C_I are purely real while B and C are purely imaginary.

B. Characteristic Impedance

The characteristic impedance, Z_u, of the ideal periodic artificial line is identical to the image impedance of its unit cell. For a symmetric unit cell [14]-[17],

$$Z_u = R_u + j\ X_u = \sqrt{B/C} \tag{5}$$

with $Z_u=R_u$ in the passbands and $Z_u=jX_u$ in the stopbands. For a symmetrical T-section ($Z_b = \infty$, $Y_d = 0$) [17]

$$Z_u = \sqrt{Z_a\left(Z_a + 2/Y_c\right)}, \tag{6}$$

for a symmetrical Π-section ($Z_a = \infty$, $Y_c = 0$) [17]

$$Z_u = 1/\sqrt{Y_d\left(Y_d + 2/Z_b\right)}, \tag{7}$$

and for a symmetrical M-section ($Z_b = \infty$)

$$Z_u = \sqrt{\left(Z_a + 2/Y_c\right)/\left(Y_d\left(Y_d + 1/Z_a\right)\left(Z_a + 2/Y_c + 1/Y_d\right)\right)}. \tag{8}$$

Band-edge frequencies of the artificial line occur when sign changes occur within the square roots of the corresponding unit cell's Z_u, as is evident by inspection of the equations for Z_u in Table 1. For cells with distributed elements, band edges can also occur at frequencies where $\tan(\theta)$ changes sign, depending on the cell parameters.

C. Image Propagation, Attenuation, & Phase

The image attenuation, α_u, and the image phase, β_u, are the real and imaginary parts of the image propagation function, γ_u, of the unit cell, where [14]-[17]

$$\gamma_u = \alpha_u + j\ \beta_u = \sinh^{-1}\sqrt{BC} = 2\sinh^{-1}\sqrt{\left(\sqrt{1+BC}-1\right)/2}. \tag{9}$$

In the passbands [14]-[17], $\alpha_u = 0$ and β_u is

$$\beta_u = \sin^{-1}\sqrt{B_I\ C_I} = -2\sin^{-1}\sqrt{\left(1-\sqrt{1+BC}\right)/2}, \tag{10}$$

while in the stopbands [17], β_u is frequency-independent and a multiple of π, or odd multiple of $\pi/2$, and α_u is

$$\alpha_u = -\sin^{-1}\sqrt{BC}. \tag{11}$$

For a symmetrical T-section [17]

$$\gamma_u = 2\sinh^{-1}\sqrt{Z_a\ Y_c/2}, \tag{12}$$

for a symmetrical Π-section [17]

$$\gamma_u = 2\sinh^{-1}\sqrt{Z_b\ Y_d/2}, \tag{13}$$

and for a symmetrical M-section

$$\gamma_u = 2\sinh^{-1}\sqrt{\left(Z_a Y_c + 2Z_a Y_d + \left(Z_a Y_c\right)\left(Z_a Y_d\right)\right)/2}. \tag{14}$$

D. Phase

The passband phase angle, φ, of the ideal periodic artificial line is identical to the phase angle, φ_u, of the unit cell multiplied by the number of cells in the line:

$$\varphi = -n\beta_u = n\varphi_u, \tag{15}$$

$$\varphi_u = 2\sin^{-1}\sqrt{\left(1-\sqrt{1+BC}\right)/2}. \tag{16}$$

Note that $\varphi_u = -\beta_u$ and $\varphi = -\beta$ (where β is the phase constant of the periodic artificial line). From (12), for a symmetrical T-section

$$\varphi_u = 2\sin^{-1}\left(j\sqrt{Z_a\ Y_c/2}\right), \tag{17}$$

from (13), for a symmetrical Π-section

$$\varphi_u = 2\sin^{-1}\left(j\sqrt{Z_b\ Y_d/2}\right), \tag{18}$$

and from (14), for a symmetric M-section

$$\varphi_u = 2\sin^{-1}\left(j\sqrt{\left(Z_a Y_c + 2Z_a Y_d + \left(Z_a Y_c\right)\left(Z_a Y_d\right)\right)/2}\right). \tag{19}$$

The resulting unit cell phase equations provided in Table 1 are correct for the first passbands, but the sign of the phase can be in error for higher order passbands due to sign ambiguities inherent in the form of the equations. The correct sign is that for which the phase slope is negative, ensuring positive group delay.

E. Non-Ideal Terminations

When a periodic structure composed of a cascade of identical unit cells is not terminated in its frequency-dependent characteristic impedance, but, as is common, is terminated in a frequency-independent real impedance R, such as 50Ω, then the passband will suffer from loss due to the mismatched impedances. The mismatched passband loss and band-gap attenuation are represented by

$$L = 10\log_{10}\left[1-\left(\frac{Z_u}{R}-\frac{R}{Z_u}\right)^2\frac{\sinh^2(n\gamma_u)}{4}\right]\ dB, \qquad (20)$$

which in the passbands becomes [15]

$$L_P = 10\log_{10}\left[1+\left(\frac{R_u}{R}-\frac{R}{R_u}\right)^2\frac{\sin^2(n\beta_u)}{4}\right]\ dB, \qquad (21)$$

and in the band gaps becomes [16]

$$L_S = 10\log_{10}\left[1+\left(\frac{X_u}{R}+\frac{R}{X_u}\right)^2\frac{\sinh^2(n\alpha_u)}{4}\right]\ dB. \qquad (22)$$

Note that minimum passband loss occurs for $\beta = m\pi/n$ and maximum passband loss occurs for $\beta = (2m-1)\pi/(2n)$, where m is an integer [17].

There are several methods of reducing passband loss due to mismatched terminations. The simplest method is to choose $R_u=R$ at a frequency removed from the "center" of the passband such that maximum L_P is minimized [16], while a more effective method is to add impedance transformers to the ends of the periodic line such that the line impedance is transformed to more closely match the termination impedance [16],[17]. When no attempt at impedance matching is made, one can expect relatively poor passband insertion loss and return loss, as demonstrated by the highpass lines in [7, Fig. 3].

The most promising alternative for designing a well-matched artificial transmission line is to abandon a periodic structure altogether and employ modern filter synthesis [e.g., 18] to realize an artificial line with optimum frequency and loss characteristics for a given number of components. However, if other considerations force a cascaded unit-cell approach, hopefully the information in this paper and in [11]-[17] will be of use.

III. Conclusion

Image-parameter filter theory is a convenient tool for investigating the frequency dependence of periodic transmission structures composed of cascades of identical unit cells. Some aspects of image parameter theory have been reviewed, and, using image parameter approaches, properties of a variety of simple left-handed and right-handed unit-cell circuit structures have been tabulated. However, if economy and performance are valued, artificial-transmission-line designers would do well to consider abandoning periodic image-parameter filters terminated by mismatched impedances, as filter designers have, in favor of non-periodic filter structures synthesized for prescribed termination impedances and a prescribed frequency and/or phase response using a minimum number of components.

References

[1] C. M. Krowne, "Electromagnetic-field theory and numerically generated results for propagation in left-handed guided-wave single-microstrip structures," IEEE Trans. Microwave Theory Tech., **51**, pp. 2269-2283, Dec. 2003.

[2] C. M. Krowne, "Physics of propagation in left-handed guided wave structures at microwave and millimeter-wave frequencies," Phys. Rev. Lett., **92**, 053901, Feb. 6, 2004.

[3] G. V. Eleftheriades, A. K. Iyer, and P. C. Kemer, "Planar Negative Refractive Index Media Uisng periodically L-C Loaded transmission lines," IEEE Trans. Microwave Theory Tech., **30**, pp. 2702-2712, Dec. 2002.

[4] S. Ramo, J. R. Whinnery, and T. Van Duzer, *Fields and Waves in Communication Electronics*, John Wiley & Sons, 1965, pp. 51-53 and 737-740.

[5] C. Caloz and T. Itoh, "Application of the transmission line theory of left-handed (LH) materials to the realization of a microstrip "LH line"," IEEE-APS Int'l Symp., **1**, pp. 412-415, San Antonio, TX, June 2002.

[6] C. Caloz and T. Itoh, "Novel microwave devices and structures based on the transmission line approach of meta-materials," *2003 IEEE MTT-S Int. Microwave Symp. Dig.*, pp. 195-198, June 2003.

[7] A. Sanada, C. Caloz, and T. Itoh, "Characteristics of the composite right/left-handed transmission lines," IEEE Microwave Wireless Comp. Lett., **2**, pp. 68-70, Feb. 2004.

[8] I-H. Lin, M. DeCincentis, C. Caloz, and T. Itoh, "Arbitrary dual-band components using composite right/left-handed transmission lines," IEEE Trans. Microwave Theory Tech., **52**, pp. 1699-1713, April, 2004.

[9] A. Gomez, M. A. Solano, A. Lakhtakia, and A. Vegas, "Circular waveguides with Kronig-Penney morphology as photonic band-gap filters," Microwave Opt. Tech. Lett., **37**, pp. 316-321, June 5, 2003.

[10] L. Zhu, "Guided-wave characteristics of periodic coplanar waveguides with inductive loading – unit-length transmission parameters," IEEE Trans. Microwave Theory Tech., **51**, pp. 2133-2138, Oct. 2003.

[11] G. A. Campbell, "Physical theory of the electric wave-filter," B.S.T.J., **1**, no. 2, pp. 1-32, Nov. 1922.

[12] O. J. Zobel, "Theory and design of uniform and composite electric wave-filters," B.S.T.J., **2**, no. 1, pp. 1-46, Jan. 1923.

[13] W. P. Mason and R. A. Sykes, "The use of coaxial and balanced transmission lines in filters and wide-band transformers for high radio frequencies," Bell Systems Tech. J., **16**, pp. 275-302, 1937.

[14] E. A. Guillemin, Communication Networks, Vol. II, New York, NY: John Wiley & Sons, 1935.

[15] P. I. Richards, "Applications of Matrix Algebra to Filter Theory," *Proc. IRE*, pp. 145P-150P, March 1946.

[16] Harvard Radio Research Laboratory Staff, *Very High-Frequency Techniques, Vol. II*, New York, NY: McGraw-Hill, 1947, Ch. 26 & 27 by S. B. Cohn.

[17] G. Matthaei, L. Young and E. M. T. Jones, *Microwave Filters, Impedance-Matching Networks, and Coupling Structures*, Dedham, MA: Artech House, 1980, Ch. 2 & 3.

[18] I. Hunter, *Theory and Design of Microwave Filters*, London: IEE, 2001.

[19] H. W. Bode, *Network Analysis and Feedback Amplifier Design*, New York, NY: Van Nostrand, 1945, Ch. 1.

Table 1.

Properties of some three-element T and Π unit-cell circuits.

ID	Schematic	Characteristic Impedance $Z_u = Z_{oo}(\omega)\sqrt{F(\omega)}$		Phase, φ_u	Radian Cutoff Frequencies	Equivalent Transmission Line Elements
		$Z_{oo}(\omega)$	$F(\omega)$			
R_{LT}	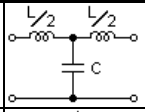	$\sqrt{\frac{L}{C}}$	$1-\left(\frac{\omega}{\omega_1}\right)^2$	$-2\sin^{-1}\left(\frac{\omega}{\omega_1}\right)$	$\omega_1=\frac{2}{\sqrt{LC}}$	
$R_{L\Pi}$	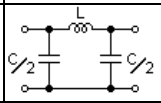		$\frac{1}{1-\left(\frac{\omega}{\omega_1}\right)^2}$			
L_{LT}	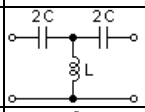		$1-\left(\frac{\omega_2}{\omega}\right)^2$	$2\sin^{-1}\left(\frac{\omega_2}{\omega}\right)$	$\omega_2=\frac{1}{2\sqrt{LC}}$	
$L_{L\Pi}$	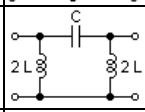		$\frac{1}{1-\left(\frac{\omega_2}{\omega}\right)^2}$			
R_{QT}	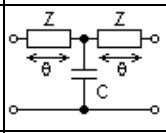	Z	$\frac{1-\left(\frac{\omega}{\omega_{11}}\right)^2}{1-\left(\frac{\omega}{\omega_{12}}\right)^2}$	$-2\sin^{-1}\left(\left(\frac{\omega}{\omega_{11}}\right)\sqrt{\frac{1-\left(\frac{\omega}{\omega_{12}}\right)^2}{\left(\frac{\omega}{\omega_{11}}\right)^2-\left(\frac{\omega}{\omega_{12}}\right)^2}}\right)$	$\omega_{11}=\frac{2}{\sqrt{L_{11}C}}$ $\omega_{12}=\frac{2}{\sqrt{L_{12}C}}$ $\omega_3=\frac{k\pi}{2}\left(\frac{v}{l}\right)$	$L_{11}=\frac{2Z\tan(\theta)}{\omega}$ $L_{12}=\frac{-2Z}{\omega\tan(\theta)}$ $C_{11}=\frac{2\tan(\theta)}{\omega Z}$
$R_{Q\Pi}$	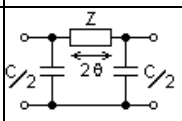		$\frac{1}{\left(1-\left(\frac{\omega}{\omega_{11}}\right)^2\right)\left(1-\left(\frac{\omega}{\omega_{12}}\right)^2\right)}$			
L_{QT}	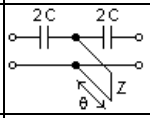	$\sqrt{\frac{L_{21}}{C}}$	$1-\left(\frac{\omega_{21}}{\omega}\right)^2$	$2\sin^{-1}\left(\frac{\omega_{21}}{\omega}\right)$	$\omega_{21}=\frac{1}{2\sqrt{L_{21}C}}$ $\omega_4=\frac{(2k-1)\pi}{2}\left(\frac{v}{l}\right)$	$L_{21}=\frac{Z\tan(\theta)}{\omega}$
$L_{Q\Pi}$	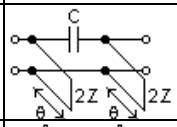		$\frac{1}{1-\left(\frac{\omega_{21}}{\omega}\right)^2}$			
R_{DT}	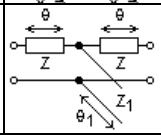	Z	$\frac{1-\left(\frac{\omega}{\omega_{13}}\right)^2}{1-\left(\frac{\omega}{\omega_{14}}\right)^2}$	$-2\sin^{-1}\left(\left(\frac{\omega}{\omega_{13}}\right)\sqrt{\frac{1-\left(\frac{\omega}{\omega_{14}}\right)^2}{\left(\frac{\omega}{\omega_{13}}\right)^2-\left(\frac{\omega}{\omega_{14}}\right)^2}}\right)$	$\omega_{13}=\frac{2}{\sqrt{L_{11}C_1}}$ $\omega_{14}=\frac{2}{\sqrt{L_{12}C_1}}$ $\omega_3=\frac{k\pi}{2}\left(\frac{v}{l}\right)$	$L_{11}=\frac{2Z\tan(\theta)}{\omega}$ $L_{12}=\frac{-2Z}{\omega\tan(\theta)}$ $C_1=\frac{\tan(\theta_1)}{\omega Z_1}$
$R_{D\Pi}$	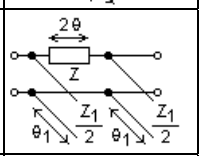		$\frac{1}{\left(1-\left(\frac{\omega}{\omega_{13}}\right)^2\right)\left(1-\left(\frac{\omega}{\omega_{14}}\right)^2\right)}$			
R_{TT}	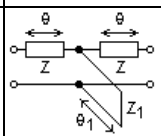		$\frac{1-\left(\frac{\omega}{\omega_{15}}\right)^2}{1-\left(\frac{\omega}{\omega_{16}}\right)^2}$	$-2\sin^{-1}\left(\left(\frac{\omega}{\omega_{15}}\right)\sqrt{\frac{1-\left(\frac{\omega}{\omega_{16}}\right)^2}{\left(\frac{\omega}{\omega_{15}}\right)^2-\left(\frac{\omega}{\omega_{16}}\right)^2}}\right)$	$\omega_{15}=\frac{2}{\sqrt{L_{11}C_2}}$ $\omega_{16}=\frac{2}{\sqrt{L_{12}C_2}}$ $\omega_3=\frac{k\pi}{2}\left(\frac{v}{l}\right)$	$L_{11}=\frac{2Z\tan(\theta)}{\omega}$ $L_{12}=\frac{-2Z}{\omega\tan(\theta)}$ $C_2=\frac{-1}{\omega Z_1\tan(\theta_1)}$
$R_{T\Pi}$	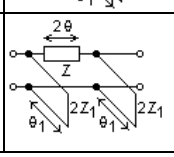		$\frac{1}{\left(1-\left(\frac{\omega}{\omega_{15}}\right)^2\right)\left(1-\left(\frac{\omega}{\omega_{16}}\right)^2\right)}$			

Note: k is an integer and $\theta = \omega l/v$ and $\theta_1 = \omega l_1/v_1$, where l and l_1 are physical lengths, and v and v_1 are propagation velocities, of the transmission line segments with characteristic impedances Z and Z_1.